

## Review

# The properties and the effect of operating parameters on nickel plating (review)

**Oluranti Sadiku-Agboola\*, Emmanuel Rotimi Sadiku and Olusesan Frank Biotidara**

Department of Mechanical Engineering, Faculty of Engineering and the Built Environment, Tshwane University of Technology, Pretoria, South Africa. CSIR Campus building 14D, Postnet Suite # 186 Private Bag x025 Lynnwoodridge 0040, Republic of South Africa.

Accepted 28 December, 2011

**The energy required in an electroplating process and the material costs are important considerations in product manufacturing. The most important plating criteria, however, are quality and the uniformity of the deposited metals. The nickel plating process is used extensively for decorative, engineering, and electroforming purposes. Because of the appearance and other properties of the electrodeposited material, nickel deposition can be varied, over a wide range, by controlling the composition and the operating parameters of the plating solution. Decorative applications account for about 80% of the nickel consumed in plating; 20% is consumed for engineering and electroforming purposes. Autocatalytic (electroless) nickel plating processes are commercially important but are outside the scope of this review. In this review, the basic facts of nickel electroplating processes, thickness test and methods, are discussed. The properties of nickel and the different effects of the operating parameters on nickel plating, together with the simulation and design tools, are also reviewed. Simulation tools can help to obtain better plating results. Non-destructive techniques to evaluate the coatings on a microstructural and the technical evaluation with TEM, SEM, XRD and other techniques were also reviewed.**

**Key words:** Electroplating, nickel plating, metal distribution, nickel thickness, electroforming and thickness test.

## INTRODUCTION

Electroplating is widely used to coat a metal, with a thin layer of another metal. Nickel electroplating is becoming an increasingly versatile process used for surface finishing processes that have a broad spectrum of end use that includes decorative, engineering and electroforming applications. Of the various electrodeposited metals, nickel is one of the most often employed to increase the corrosion resistance or electrical conductivity of the underlying substrate (Sung-Ting et al., 2008). Nickel plating for engineering purposes are usually from solutions that deposits pure nickel. The most important property in engineering end uses is, generally corrosion resistance, but wear resistance, solderability, and

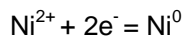
magnetic and other properties may be relevant in specific applications. Electroforming is a specialized use of the electroplating process in which nickel is deposited and subsequently removed from a mandrel to yield an all-nickel component or article. Electroformed nickel products, such as molds, dies, record stampers, seamless belts, and textile printing screens are important commercial products. The processes, used for decorative, engineering and electroforming purposes are described subsequently, following the revision of some basic facts about the nickel-plating process, the thickness test, nickel plating properties and simulation tools and design.

## BASIC CONSIDERATION

Nickel plating is the electrolytic deposition of a layer of

\*Corresponding author. E-mail: [sadikuo@tut.ac.za](mailto:sadikuo@tut.ac.za), [f.unmi2406@gmail.com](mailto:f.unmi2406@gmail.com).

nickel on a substrate. The process involves the dissolution of one electrode (the anode) and the deposition of metallic nickel on the other electrode (the cathode). Direct current is applied between the anode (positive) and the cathode (negative). Conductivity between the electrodes is provided by an aqueous solution of nickel salts. When nickel salts are dissolved in water, nickel is present in solution as divalent, positively charged ions ( $\text{Ni}^{2+}$ ). When current flows, divalent nickel ions react with two electrons ( $2e^-$ ) and are converted to metallic nickel ( $\text{Ni}^0$ ) at the cathode. The reverse occurs at the anode where metallic nickel dissolves to form divalent ions: The electrochemical reaction in its simplest form is:



Nickel plating process can be operated for a long period of time without interruption because the nickel ions discharged at the cathode are replenished by the nickel ions formed at the anode.

### Metal distribution

Industrial production requires coating on several parts in the same electrolytic tank. The main difficulty is to obtain a uniform deposit on each part and from part to part in order to satisfy tolerances assigned by the performance specification (Druesne et al., 2000). It is always good to apply uniform thickness of nickel on all significant surfaces to meet the plating specifications that require minimum coating thickness values at specified points on the surface. One of the most important quality parameters of an electroplated coating is the uniformity of metal distribution over the article surface. The uniformity depends on the configuration of an electrolytic cell (shape, size, and relative position of electrodes) and on the electrochemical component (polarization phenomena) (Karavaev et al., 2006). The amount of metal that deposits on the surface of any object being plated is proportional to the current that reaches the surface. The thickness of the deposit at the cathode and the distribution of the coating can be controlled by adequate racking and placement of the parts in solution, and by the use of thieves, shields, and auxiliary anodes. Parts can be designed to minimize problems. It may be necessary to deposit more nickel than is specified in order to meet a minimum thickness requirement on a specific article. The nickel processes used for decorative, engineering and electroforming purposes have the same electrochemical reaction. The weight of nickel deposited at the cathode is controlled by natural laws that make it possible to estimate the thickness of the nickel deposited. These estimates must be adjusted to account for variations in cathode efficiencies for specific processes. Normally, cathode efficiency values are between 93% and 97% for most nickel processes. Some fast bright nickel-plating

processes may have lower efficiencies. The actual thickness at any point, on a shaped article, depends on current flow. In practice, it is necessary to measure coating thickness on actual parts and make necessary adjustments to racks, thieves, and/or shields before thickness can be controlled within a specified range.

### Estimation of nickel thickness

The amount of nickel that is deposited at the cathode is determined by the product of the current (in amperes) and the time (in hours). If the area being plated is known, the average thickness of the nickel coating can be estimated (Thickness equals the weight of nickel divided by the product of the area and the density of nickel. It is important to use consistent units. Nickel has a density of  $0.322 \text{ lb/in}^3$ ). Because a small percentage of the current is consumed at the cathode in discharging hydrogen ions, the efficiency of nickel deposition is less than 100%. This fact must be taken into account in estimating the weight and the thickness of nickel that will be deposited under practical plating conditions. Table 1 is a data sheet on nickel deposition, based on 96.5% cathode efficiency. The table relates coating thickness, weight per unit area, current density, and time of plating. Anode efficiency is normally 100%. Because anode efficiency exceeds cathode efficiency by a small percentage, nickel-ion concentration and pH will rise as the bath is used. Drag-out of nickel-plating solution may compensate for nickel metal build-up in solution to some extent, but at some point, it may be necessary to remove a portion of solution from the plating tank and replace the solution removed with water and other constituents. The pH of the solution is normally maintained by adding acid.

Researchers have used some numerical methods to estimate thickness of metals. Haimovich et al. (1996) presented a technique based on combination of backscattered electron image analysis with Monte Carlo simulation of backscatter process to estimate and measure the thickness of thin surface layers in the approximate range of  $1 \times 10^{-3} \mu\text{m}$  to  $1 \mu\text{m}$  depending on the material. Zhang et al. (2007) reported the finite element method simulation of deep-drawing of steel sheet with nickel coating based on the solid element and dynamic explicit method. Penalty function method was used to treat the contact algorithm. The friction between punch and coating sheet was based on a coulomb formulation. The combination of coating and substrate was defined as tied with failure contact. Kaneko et al. (2006) investigated the influence of additives on the filling process of via holes in damascene electroplating with the use of a kinetic Monte Carlo method. The basic system is the solid-by-solid model for crystal growth which includes the vacancy formation during the growth of thin film. Three kinds of additives are included in the model in order to control the local surface growth rate. Inhibitors

**Table 1.** Nickel electroplating solutions (Davis, 2000).

Parameter	Watts nickel	Nickel sulfamate	Typical semibright bath
<b>Electrolyte compositions (g/l)</b>			
Nickel sulfate, NiSO <sub>4</sub> .6H <sub>2</sub> O	225 to 400	-	300
Nickel sulfamate, Ni(SO <sub>3</sub> NH <sub>2</sub> ) <sub>2</sub>	-	300 to 450	-
Nickel chloride, NiCl <sub>2</sub> .6H <sub>2</sub> O	30 to 60	0 to 30	35
Boric acid, H <sub>3</sub> BO <sub>3</sub>	30 to 45	30 to 45	45
<b>Operating conditions</b>			
Temperature (°C)	44 to 66	32 to 60	54
Agitation	Air or mechanical	Air or mechanical	Air or mechanical
Cathode current density (A/dm <sup>2</sup> )	3 to 11	0.5 to 30	3 to 10
Anodes	Nickel	Nickel	Nickel
pH	2 to 4.5	3.5 to 5	3.5 to 4.5
<b>Mechanical properties</b>			
Tensile strength (MPa)	345 to 485	415 to 610	-
Elongation (%)	10 to 30	5 to 30	8 to 20
Vickers hardness (100 g/load)	130 to 200	170 to 230	300 to 400
Internal stress (MPa)	125 to 210 (tensile)	0 to 55 (tensile)	35 to 300 (tensile)

and levellers have the effect of preventing the deposition, while accelerators increase the local growth rate. Levellers are modeled to stick to the tips of the surface. A series of simulations by changing the parameters which characterize the additives in order to observe their influence on the filling mechanism were performed. Mathias and Chapman (Mathias and Chapman, 1990) used two the dimensional models to measure the radial variations of composition and thickness of electro-deposited zinc-nickel alloys on a rotating disk electrode. These measurements were made for deposits obtained at steady state from chloride electrolytes at different bath compositions, electrode rotation rates, and applied voltages. The two-dimensional transport model, which accounts for migration and complexation of the zinc by chloride, was used to calculate the radially dependent interfacial concentration and potential profiles for each set of experimental conditions. The calculated profiles and the experimental data were compared in order to estimate the unknown parameters in a postulated electrode kinetics model for the code position processes. The physical and mechanical properties of nickel deposited from Watts solutions are affected by the operating conditions and chloride content. Table 1 gives nickel electroplating solutions.

## THICKNESS TEST

Because of the fact that corrosion resistance has often been shown to be closely related to thickness of the deposit, the requirement of minimum thickness in a

product specification is obvious. However corrosion resistance is the only criterion that makes thickness specification necessary and functional requirement is also of equal importance. Many products are plated to achieve definite physical and chemical properties such as conductivity on printed wiring boards and other electronic devices. Plating specific coatings greatly enhances the functions of particular items and there are minimums and maximums in plating thickness specifications which must be followed in order to for item to perform as designed. Few instruments are popularly used these days to read thickness directly. Beside the micrometer, microscopic cross sectioning is the most commonly used direct method. It is more accurate and relatively more sophisticated. All other instruments that are also used vary in the degree of accuracy and sophistication and taking ingenious advantage of differences in the physical and chemical properties of the coating and substrate. Because of the variety of coatings and basic material combinations used today, there are different testing devices. Each method takes advantage of the unique characteristics of a particular coating substrate system. Following are some of the coating instruments/methods.

## Microscopic-optical methods

For many years, microscopic cross-sections were considered the referee method when thickness tests by other means were in dispute; but for thickness under 2  $\mu\text{m}$ , this method is unreliable. Some researchers had reported an error of ~50% in viewing deposits in order of

1  $\mu\text{m}$  thick. The limiting number for any degree of acceptable accuracy is 2  $\mu\text{m}$ . The accuracy and reliability of microscopic method depend on the skills and technique of operator.

### Chemical methods

Most individual techniques fall under this heading. They include: Dipping, jets, gas evolution, dropping and drop methods. Dipping method, like the well known, Preece test, where zinc coated steel specimens were dipped in a neutral copper sulfate solution, are inconsistent to modern electroplating, as are the jet and gas evolution test. This is because there are better and more reliable methods that are readily available. The dropping test method consists of applying corrosive solution at a constant dropping rate to an electroplated surface, and with a stop watch measuring the time it takes to penetrate the coating and expose the substrate. The time it takes for the coating to be penetrated is proportional to the coating thickness. This test is used for electrodeposited zinc, tin copper cadmium coating.

### Magnetic method

Magnetic method of measuring electrodeposits thickness are very popular because the instruments used are relatively cheap, the test is non-destructive. It can be adapted to highly localized measurements. The main disadvantage of this method is the necessity of having a magnetic coating, a magnetic and basis metal, or both, such as electrodeposited nickel on steel. Common measuring combinations are paints, plastic, copper, nickel, chromium; etc. Nickel can be measured on most substrate with varying results due to the permeability variations of the nickel coating. With multiple plates such as copper and silver on steel, only the combined plates can be read. The way to read a combination such as this, magnetically, is to first read the copper and then subtract the copper reading from the total to determine the silver thickness. Because the various devices actually measure the magnetic attraction between a magnet and the object coating substrate combination, or the reluctance of a magnetic flux path passing through the coating and the substrate with reluctance being the magnetic resistance, the instrument must be calibrated against standards of known thickness (Druesne and Afzali, 2003). Precise calculation cannot be stressed too strongly because there are many physical and structural factors of the coating and substrate which may affect the magnetic properties of either or both. It is for this reason that calibration standards should be identical to the specimens undergoing thickness examination. With nickel, the physical properties of the deposit will affect the accuracy of the test. Plating conditions, plate composition and particularly, stress in the deposit will affect the results. With

suitable heat treatment stress can be relieved, prior to making a thickness determination. A heat treatment of 400°C for 30 min will equalize the magnetic permeability of a dull watts nickel. Multi-layered nickel deposits can give erroneous results, because each layer is of a different composition with different magnetic properties.

### Eddy current

Just as magnetic type instruments measure reluctance which must be calibrated against thickness standards, eddy current devices measure impedance, which, must also be calibrated against thickness standards in order to render meaningful thickness measurements, with the impedance, being the conductor. There is a great similarity between the magnetic and eddy current type instruments; so much that several companies now manufacture a dual instrument. An eddy current generates a high-frequency electric field in a coil mounted in an open ferrite pot core. When the probe is placed on a specimen with a metallic substrate, eddy currents are induced in the metal. The magnitude of the eddy currents depends primarily upon the distance between the metal surface and the probe; the distance being equivalent to the insulating coating thickness, or if a metal, the plating thickness. The strength of the induced current is indirectly measured through the interaction of its magnetic field with the probe coil. The changes in the probe coil are measured with a micro-ammeter and are related to the coating thickness through the use of a calibrated reference coating thickness standard.

Eddy currents are affected by the frequency applied to the coil, the electrical conductivity of the sample, its magnetic permeability and the heat treatment history of the basis metal. The higher the frequency of the applied AC to the coil, the shallower will be the penetration of the eddy currents in any given material. Thus, lower frequencies are used for the thicker coatings. The difference in conductivity between coating and substrate is what actually makes this instrument a thickness gauge. This is because it measures the difference in conductivity between the two. The conductivity of a plated metal can be influenced by solution composition, brighteners and addition agents together with current density at which it was plated. Eddy current instruments are fairly accurate to within  $\pm 10\%$  at thickness in excess of 5  $\mu\text{m}$  (Druesne and Afzali, 2003).

### Mass per unit area

The measurement of the mass per unit area is considered the most accurate means for detecting thickness. There are a number of methods used to determine mass per unit area, the most common being weight gain, coulometric, and actually counting the number of atoms in a specific area by bombarding it with X-rays and beta

rays. However, coating is often weighed in a designated area; thickness is derived by dividing the mass per unit area by density, which is mass per unit volume. Sometimes the addition agents added to the plating process to modify or give the deposit certain properties, often intrude the deposit and thereby change its density. Begis and Babadzhinov (1996) analyzed the potentialities of the coulometric method of thickness measurement. The design features and technical capabilities of the Limeda DEM micro-coulometric thickness gauge were considered. The gauge can be used for measurements on a small area ( $1 \text{ mm}^2$ ) with a rapid rate of electroetching ( $0.5 \text{ } \mu\text{m/s}$ ). Slepushkin et al. (2005) also reviewed the improvement in the design of electrochemical coating thickness gauge and electrochemical surface analyzer. The analytical procedure and equipment were continuously refined. They reviewed new and developed techniques of electrochemical analysis.

### Weight gain method

The weight of a coating is obtained in several ways, in relation to the techniques used. A plated specimen of known area is weighed, and the plating is removed by a suitable stripper that does not attack the basis metal, which is then reweighed. From the difference in weight, the area and the density of the plated coating, the thickness can be readily calculated (Durney, 1984). Another method, modified slightly and used when a suitable solvent cannot be found, is to weigh a specimen of a known area before plating, and then weigh again after plating. From the difference in weight, known area and density of the material, the thickness can be calculated.

All of these methods will only give an average thickness of the whole specimen; the weight gain method by using plating techniques is capable of supplying standards for the calibration of many sophisticated testing instruments.

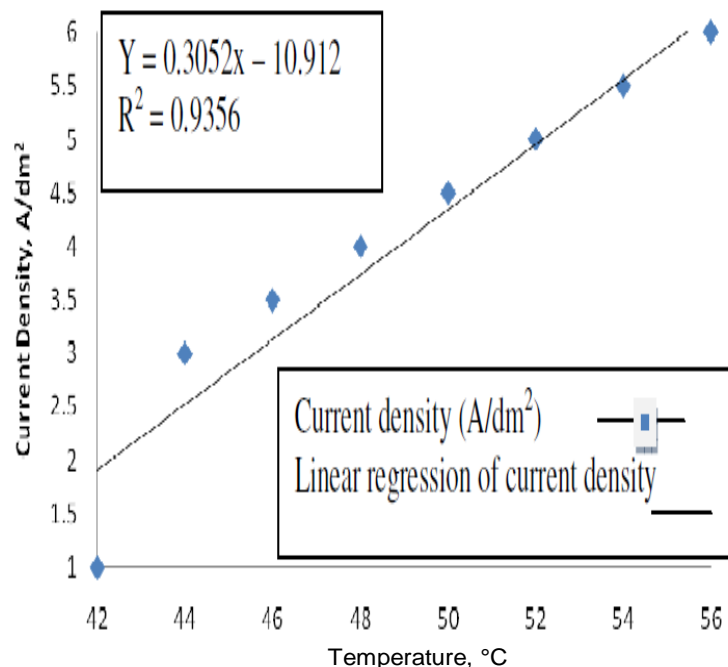
### PROPERTIES OF ELECTROPLATED NICKEL

Property measurements of electrodeposited nanocrystalline metals and alloys have revealed improved performance and in some cases, unique properties over conventional materials with the same chemical composition. Increased hardness, improved corrosion and wear resistance, lower coefficients of friction and enhanced solid solubility make nanostructured metals and alloys ideal candidates for many industrial applications. Properties of electroplated nickel such as crystallographic texture, Young's modulus, strength and microstructure strongly depend on the parameter: mean current density used for electrodeposition. Different nickel electroplating solutions produce coatings with different levels of internal mechanical stress and ductility. The lowest stress and maximum ductility are provided by nickel sulfamate

solutions. Brittle coatings are caused by excessive concentrations of organic agents (levelers, brighteners), decomposition products of brighteners, nickel chloride and metallic contaminants. Kim (2006) addressed a relatively simple method of measuring the mechanical properties such as Young's modulus and residual stress of electroplated Ni thin film using the resonance method of atomic force microscope. The measured Young's modulus of nickel at the end of each plating step ranged from 148.04 to 159.90 GPa with the maximum standard deviation of 3.47. Baek et al. (2004) characterized the mechanical properties of electroplated nickel thin film using two methods: Tension test and nano-indentation test. In the tension test, a linearly guided motor was used as actuator and the applied force was measured using a load cell. In the indentation test, elastic module was measured using a CSM (continuous stiffness measurement) module. Fritz et al. (2002) determined the material mechanical parameters by means of micro tensile testing. At low mean current density ( $\sim 2 \text{ mA/cm}^2$ ), brittle layers with high Young's modulus and high strength were obtained, whereas at high current density ( $\sim 15 \text{ mA/cm}^2$ ), ductile layers with low Young's modulus and low strength were deposited. Jun Tang et al. (2010) used different electrolytes to fabricate nickel structures in MEMS devices by the LIGA or UV-LIGA process to meet different requirements. In order to investigate the microstructure and mechanical properties of nickel thin films electroplated in different electrolytes, four sets of nickel specimens were fabricated in different electrolytes: Sulfamate bath with both saccharine and butynediol added (type A-I); sulfamate bath with saccharine added (type A-II); watts bath with saccharine added (type B); and chloride bath with saccharine added (type C). The function of these additives was to obtain the stress-free nickel films. The specimens were measured in our uniaxial tensile test system; their surface morphology and fractography, microstructure and texture were studied by scanning electron microscope (SEM), transmission electron microscope (TEM) and X-ray diffraction (XRD), respectively. The results show that the four sets of specimens have different mechanical properties and microstructures. The tensile strengths of the type A-II, type C and type A-I specimens, increase with decreasing grain size, which is in accordance with the Hall-Petch law. In contrast, type B specimens have the highest value of ultimate tensile strength and elongation, but with the largest grain size among all the specimens. The XRD results show that there is no preferred orientation in type B while others have a preferred lattice orientation in (200) along the growth direction. This might be the reason for the difference between type B and other types.

### Effect of operating parameters on nickel plating

Luo et al. (2006) systematically investigated the properties



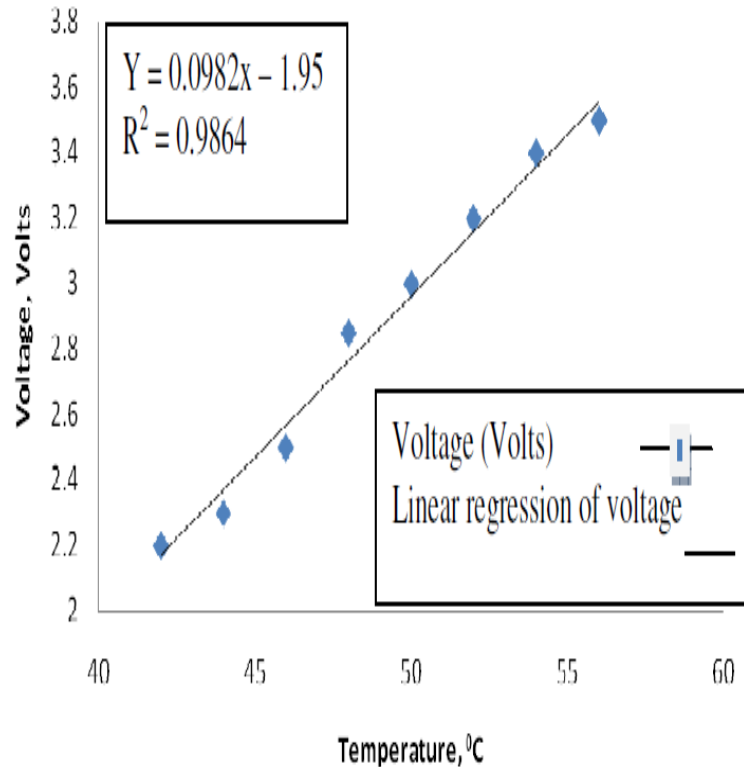
**Figures 1.** The effect of temperature on current density on ionic solution of nickel (Sadiku-Agboola et al., 2011).

of electroplated Ni thin films as a function of plating temperature and current density. The resistivity and its temperature coefficient remain unchanged on varying the process conditions, though the values of these properties are approximately three times and one-half of those of bulk Ni material, respectively. Optimal conditions of  $J = 2 \text{ mA/cm}^2$  and  $60^\circ\text{C}$  were found for stress-free Ni thin films. The modulus of elasticity of the Ni films is as high as that of bulk Ni (210 GPa) when plated at high temperature and low current density, and then decreases linearly with increasing plating current density; down to 85 GPa at a plating current density of  $30 \text{ mA/cm}^2$ . It was believed that higher plating rates produced fine-grained structures of low density, leading to a high tensile stress and low modulus of elasticity, while lower plating rates produced a dense material with a modulus of elasticity and a compressive residual stress, close to that of bulk Ni. A clear correlation between modulus of elasticity and stress exists, which reveals that a material under high tensile stress may possess a low modulus of elasticity, and is not suitable for fabrication of micro-electro-mechanical systems devices. Kim and Kang (2008) addressed a relatively simple method to investigate the sensitivity of Young's modulus to the plating conditions such as the plating temperature and applied current density.

This method uses the resonance method of atomic force microscope, which does not require specially microfabricated cantilevers and additional experimental set-up. The measured Young's modulus is as high as that

of bulk nickel at low plating temperature between  $40$  and  $60^\circ\text{C}$  and low applied current density ( $J = 8.6 \text{ mA/cm}^2$ ), but drastically drops at high temperature or current density. The dependence of Young's modulus on the plating thickness (less than few microns) is negligible in thin film. Razeeb et al. (2009) investigated the magnetic properties of electroplated nickel nanowires with very distinct nanostructures, which are obtained by simply changing the plating temperature of the electrolyte. Low temperature ( $40^\circ\text{C}$ ) resulted in larger average grain size comparable to the diameter of the wires, whereas higher temperature ( $60^\circ\text{C}$ ) revealed self-similar morphology composed of nanogranules. Sadiku-Agboola et al. (2011) electrolytically applied bright nickel deposits on steel in the nickel Watts bath. The effect of some operational parameters on metal deposition in bright nickel plating was investigated. Their investigation indicated that the weight of bright nickel deposited on metal during the process of electroplating was affected by plating temperature, voltage, current density, plating bath pH and plating time.

Sadiku-Agboola et al. (2011) investigation indicates that the temperature increases as the current density increases as shown in Figure 1. This was expected because higher temperature reduced the viscosity of the solution and thus offered less resistance to the movement of ions to form current. The surface morphology is influenced by the current density, the concentration of nickel salts in the bath and the type of current applied. The increase in current density improved the amount of



**Figures 2.** The effect of temperature on voltage on ionic solution of nickel (Sadiku-Agboola et al., 2011).

weight of electro-deposited, thus increased the thickness of nickel deposit. Figure 2 shows that there is a clearer correlation between temperature and voltage, as the temperature increases with increasing voltage, with a coefficient of fit of  $\approx 99\%$ .

## SIMULATION AND DESIGN TOOLS

The design of an electroplating rack requires many preliminary steps, including the choice of electrolyte and the location, shape and number of electrodes, masks and current thieves (Durney, 1984). These parameters affect deposit thickness and plating distribution. Most often the preliminary steps taken to optimize electroplating process are time-consuming if they are performed in a trial and error fashion, e.g. plating parts, measuring thickness, and plating again, etc. Accurate simulation of these trial and error can result in large gain of overall plating cost reduction. Plating part requires several parts been placed in the same electrolytic plating tank. The main difficulty is to obtain uniform deposit on each part to satisfy plating thickness tolerance assign by the performance specification. It is important to deposit more metal on a given area to achieve the necessary minimum plating thickness in another area. This increases the overall cost and also requires additional remedies in area where there is an

excess of plating metal; thus the effective electrolytic plating thickness simulation tools helps plating industries to design the most appropriate racks and tools to produce the best deposit uniformity on each part of the specimen. These tools have been designed to optimize electroplating cells and racks. An accurate analysis is required to determine distribution of deposited thickness, current densities and electrode potentials. A good plating simulation tool can help an engineering team to find the most reliable rack configuration based on the geometrical description of rack, the parts to be plated and from calculation of the electrochemical properties of the process being studied. Many industrial electroplating applications have been optimized by the use of new plating simulation software. The software is based on an original numerical method called boundary element analysis. For the last 20 years, the reliability of this kind of engineering tool and the accuracy of the results achieved have been proven by the many industrial applications (Durney, 1984).

Pertinent simulations of micro-electromechanical systems using powerful computer-aided design tools depend on a systematic characterization of the electrical, optical, magnetic, and mechanical properties of the different materials involved in the fabrication of microdevices. Basrou and Robert (2000) focused their attention on the residual stresses, which may be responsible for the

degradation of the mechanical performances of micro-actuators and sensors. In their paper, a detailed investigation of the residual stresses arising during nickel electroplating used in the LIGA technique was reported. X-ray analysis and, in particular, the  $\sin^2 \psi$  method allow a local characterization of the structural properties of the material as well as the residual stress tensor. The experimental results on their nickel plates obtained with a nickel sulphamate electrolyte show that the structural properties and the residual stresses are tightly linked to the nature of the substrates used for the depositions (silicon and copper), the densities of current, and the amount of  $\text{NiCl}_2$  in the bath and the thickness of the layers. In order to obtain the intrinsic stresses, the thermoelastic contribution to the global stresses was estimated with a finite element method and subtracted from the experimental values. In the final part of their work, they presented the effect of residual stresses in the mechanical behaviour of a microgripper fabricated by LIGA.

### Model of a rack

Electroplating process energy and material costs are very important considerations in product manufacturing. The most important plating criteria, however, are quality and plated uniformity of the deposited metals. Simulation tools can help to obtain better plating results. Druesne and Afzali (2003) described the plating rack and other electroplating hardware (masks or shields) by a graphical tool in a three-dimensional space. Interactive solid modelling, based on ACIS, allows plating simulation of the complex geometry of the electroplating rack and the parts to be plated. It is the principal part of the simulation tool. ACIS provides software developers and manufacturers in the underlying 3-D modeling functionality. The second feature is an electrolytic data manager composed of all the electrochemical characteristics needed to adequately simulate actual electrodeposition: electrolyte conductivity, cathodic and anodic polarization laws, cathodic efficiency law, properties of the deposited material, and the working current density. Simulation enables a quick evaluation and to determine whether there is any improvement on the initial rack configuration.

### NICKEL ELECTROFORMING

Electroforming is the fabrication of articles entirely by electrodeposition. Nickel is the popular metal for this purpose, since it can be plated in a ductile and low stressed form with moderate hardness (Ming et al., 2010). Electroforming is not a new process; it is almost as old as plating itself. What is new is the application of advanced technology to the field. Formerly, the process was, to a large measure, practiced as an art and correspondingly the results were sometime erratic. But

now, with a better understanding of electrochemistry, especially knowledge about the role of an additive in plating baths, allows close control of electroformed parts. Nickel electroforming is the electrodeposition applied to the manufacture of nickel products of various kinds, and it differs from electroplating in one major respect. In electroplating, the coating is metallurgically bonded to the substrate and is an integral part of the surface. In electroforming, nickel is deposited onto a mandrel or mold non-adherently, so that the nickel can be separated from the mandrel when it is removed from the plating solution. Electroforming application includes the fabrication of molds and dies, mesh and other products that are indispensable to operations in the textile, aerospace, communications, electronics, automotive, photocopying and entertainment industries (Durney, 1984). Electroform article, which has higher hardness and strength, both at ambient and elevated temperatures, can be produced from special solutions from which are deposited nickel whose structures are modified either by inorganic or organic chemicals present in the electroplating bath or by the presence of other metals as alloying ingredients. The working surface of the electroform article may be chromium plated after removal of the mandrel. Sometimes the thick skin of the electroform material, is backed by even thicker copper plate, which although softer than nickel, can be deposited at faster rate than most type of nickel.

Recently, many investigations have been made on electroforming. Ming et al. (2011) investigated the feasibility of a new micro-electroforming technique. A series of experiments were performed using special equipment, developed by the authors, followed by the evaluating the surface morphology of nickel micro-electroforms using a scanning electron microscope (SEM). Experimental results showed that, comparing with the conventional electroforming practices, a significant reduction in pinhole defects of the samples electroformed by the novel process was achieved. Nauenheim et al. (2010) reported on the electroforming in resistively switching nanocrosspoint devices made of a reactively sputtered  $\text{TiO}_2$  thin film between Pt and Ti/Pt electrodes, respectively. As most resistance switching materials,  $\text{TiO}_2$  needs to be electroformed before it can be switched. Their paper presents and compares current and voltage controlled electroforming with regard to the polarity. They were able to show that a current-driven electroforming with negative polarities leads to the switchable high resistive state without the need for a current compliance. These devices show an improved stability and reliability in bipolar resistive switching performance. Wei et al. (2008) applied micro-electroforming to fabricate metallic components of sensors, actuators, and other systems. Thick photoresists were used for making micromoulds for electroforming which closely relate to the quality and costs of an electroforming process. Optimized UV lithography processes are introduced for producing micromoulds in each of the resists and scanning electron microscope



(SEM) images of the moulds are presented and analyzed. They also presented electroformed nickel components from the micromoulds. Finally, applicability of the photoresists to electroforming microcomponents was discussed. Each of the resists demonstrates advantages and disadvantages to suit different applications. Li et al. (2011) compared the unipolar and periodic reverse pulse current electroforming. Bipolar pulse current in electroforming is known to result in better precision and surface finish. In their study, bipolar pulse current electroforming was introduced. The influencing parameters, such as electrolyte parameter, additives, current density, pH value, temperature and pulse current parameters have been studied. Experiments on nickel and nickel alloys electroforming on micro optical aspheric moulds have been done. The results indicated that bipolar pulse current could improve the quality and precision, reduce internal stress in micro electroforming. Lee et al. (2010) investigated the resistance switching (RS) phenomenon in epitaxial NiO (epi-NiO) films by employing different types of top electrodes (TEs). Epi-NiO showed successive bipolar RS when Pt and CaRuO<sub>3</sub> (CRO) were used as the TEs, but not when Al and Ti were used. They studied the temperature dependence of the current-voltage (*I-V*) characteristics for various TEs and resistance states in order to understand the conduction properties of TE/epi-NiO. Pristine CRO/epi-NiO showed metallic behavior, while pristine Pt/epi-NiO and Al/epi-NiO showed insulating behavior. Pt/epi-NiO and Al/epi-NiO, however, switched to a metallic or non-insulating state after electroforming. Transmission electron microscopy (TEM) images revealed the presence of a distinct stable interfacial AlO<sub>x</sub> layer in pristine Al/epi-NiO. On the other hand, the interfacial metal oxide layer was indistinguishable in the case of pristine Pt/epi-NiO and CRO/epi-NiO. Their experimental results suggested that epi-NiO has an oxygen defect on its surface and therefore the various TE/epi-NiO interfaces characterized in the study, adopted distinctive electrical states. Further, the bipolar RS phenomenon can be explained by the voltage-polarity-dependent movement of oxygen ions near the interface. Ming et al. (2011) prepared Ni deposits from a nickel sulfamate type electrolyte bath under vacuum-degassing and temperature-gradient conditions without any additives. Morphology and micro-hardness of the deposits obtained at the current density of 1, 3, 5 and 7A/dm<sup>2</sup> were examined and analyzed. Experimental results showed that the deposits obtained under vacuum-degassing and temperature-gradient conditions exhibited fewer pinhole defects and finer grain size comparing with those formed under conventional deposition conditions, and that the microhardness of the deposits was greater than that from conventional deposition conditions without additives while lower than that from conventional deposition conditions with additives. Under the vacuum-degassing conditions, electroforms had remarkably smoother surface with fewer void defects and finer grain

size, and considerably microhardness.

## NON-DESTRUCTIVE TECHNIQUES TO EVALUATE THE COATINGS ON A MICROSTRUCTURAL

Nondestructive evaluation (NDE) is entering a new era in the field of coating. The need for engineered coatings with controlled composition and microstructure is increasing because of increasing demands on the materials properties in a variety of applications such as aerospace, environment, catalysis, and electrodes. Cyclic oxidation tests have been carried out on the coated materials in order to simulate real conditions in service, thus bringing about scale cracking, spallation of the oxide scales and inducing strong evolutions in the composition and morphology of the underlying coatings (interdiffusion) (Svensson et al., 2004; Slepishkin et al., 2005). During high-temperature exposure, the microstructure of thermal barrier coatings evolves, leading to increased thermal conductivity. The oxidation resistance of Ni-based super alloys and bond coating materials in high-temperature environments is greatly dictated by their ability to preferentially form an adherent oxide scale on the metal surface. Thermogravimetric device is used to detect if the samples experience spalling during the high temperature dwell and even during cooling. Kakuda et al. (2009) described the evolution in the thermal properties of a 7 wt.% Y<sub>2</sub>O<sub>3</sub> stabilized ZrO<sub>2</sub> electron beam-physical vapor deposited (EB-PVD) thermal barrier coating with thermal cycling between room temperature and 1150°C until failure. The thermal diffusivity and conductivity of the coating were evaluated non-destructively based on the analysis of its photo thermal infrared emission. Although the coating density does not increase significantly with thermal cycling, the thermal diffusivity and conductivity of the coating increased substantially, particularly during the first 20 1 h cycles. The values then approach a limiting value. Complementary Raman spectroscopy suggested that the increase is accompanied by a reduction in the defect concentration in the coating and that there is also a correlation between the width of the Raman lines and the thermal conductivity. Most microstructural analysis of coatings has relied on qualitative correlation based on resolution-limited X-ray diffraction, and SEM with energy dispersive spectrometer (EDS).

Nanocrystalline materials of grain size < 100 nm are known to possess unique and useful properties including high strength and high hardness. They have been the subject of recent research in the past decade. Amorphous metallic materials have also being investigated for their unique properties, such as superior corrosion resistance, due to the absence of crystalline lattice and homogeneous distribution of different atoms. Typically amorphous metals have higher plasticity than nano-materials. Such properties, provided in the form of a coating layer, are desirable in a number of applications.

However, recent developments in nano- and micro-structural evaluation techniques have opened up new ventures. Thermal spray coatings with engineered nano-amorphous structure have been developed for potential use in many instrument applications. Sohn et al. (2004) discussed recent achievements in understanding the residual stress, phase constituents, and electrochemical resistance (or capacitance) of thermal-barrier coatings constituents, with an emphasis on the thermally grown oxide. Results from non-destructive evaluation by photo stimulated luminescence spectroscopy and Electrochemical impedance spectroscopy are correlated to the nano- and microstructural development of thermal-barrier coatings.

### Technical evaluation with TEM, SEM, XRD and other techniques

A full characterization of amorphous or nanostructured coatings at the microstructural level has some intrinsic difficulties associated with the lack of long range order and reference compounds, which often make difficult their study (Godinho et al., 2008). By the combination of different characterization techniques, it is possible in many cases to achieve valuable chemical and structural information. This section reviews some of the technical evaluation. Godinho et al. (2008) used three different techniques to illustrate how the combination of characterization techniques, as TEM associated to EDS or EELS, EFTEM, SEM, XPS, RBS and XRD was determinant to correlate microstructure with deposition parameters and properties in such complex systems. The coatings were deposited on silicon and AISI M2 steel substrates by magnetron sputtering under different Ar/N<sub>2</sub> gas mixtures from Ti and C targets (System 1 and 2) or a Si target (System 3). In each case, the performed characterization allowed to get a deeper understanding of the whole system and explain their mechanical response. Zheng et al. (2010) deposited Ni-based metal matrix composites (MMCs) components using Laser Engineered Net-Shaping (LENS) with Ni-coated and uncoated TiC reinforcement particles to provide insight into the influence of interfaces on MMCs. The microstructures and spatial distribution of TiC particles in the deposited MMCs were characterized using SEM and TEM, and the mechanical responses were investigated. In order to avoid the post-processing in micro tensile tests, Tang et al (2010) directly investigated a strain measuring method. The nickel tensile test specimen was electroplated in Watts solution under certain conditions. The measured Young's modulus, ultimate tensile strength and elongation are 171.5 GPa, 2.18 GPa and 13.8%, respectively. By comparing these results to that obtained by the traditional method, the new approach has been proved reliable. They used SEM to study the surface morphology and the fractography of the species. The SEM sample

platform was set to 55° inclined to the horizontal plane during the observation of the cross section of the fractured specimens. X-ray diffraction (XRD) test was carried out to study the texture of the nickel thin films. The microstructures of the nickel specimens were directly characterized by TEM bright field images and the diffraction patterns by using a TEM. Furthermore, the mean grain size of the nickel specimen measured by TEM images was about 160 nm with wide distribution. The XRD results showed that nickel thin film in their experiment has no preferred orientation in the growth direction. The dimple rupture with small micro voids has been observed after the fracture of specimen.

Lin et al. (2000) investigated microstructure and formability of ZnNi alloy electrodeposited sheet steel. ZnNi alloy electrodeposited sheet steels were made from a chloride bath using a high-speed flow cell. A Ni-rich flash coating was deposited first, upon which the ZnNi coating, with Ni contents ranging from 8 to 16 wt pct, was subsequently electrodeposited. It was demonstrated that the Ni content of the coating affects the forming properties and microstructure of the ZnNi coatings. The hardness of the ZnNi coating increased with Ni content, leading to poor formability and inferior adhesion of the coated steels, as evident from the large amount of coating loss during swift cupping and coating peel-off during low-temperature adhesion tests. On the other hand, the friction force between the coated steel and cupping die decreased with increasing Ni content. At low Ni contents of 8 wt pct, the coating had a porous equiaxed grain structure. As the Ni content increased, the coating surface changed to dense faceted morphologies. Pyramid morphology was observed for 16 wt pct ZnNi coatings. An X-ray diffraction (XRD) analysis showed that all coatings containing up to 16 wt pct Ni contained only  $\gamma$  phase. Transmission electron microscopy (TEM) observations showed the 8 wt pct Ni coating to have a fine-grained structure, which changed to a columnar structure at 16 wt pct Ni. The formation of the columnar structure was explained by the smaller amount of hydrogen discharge as the bath Ni ion concentration increased. Lin et al (2012) successfully coated a layer of Ni-Cr-Si-B-Fe alloy on plain steel substrate by hot dipping process. The Ni-Cr-Si-B-Fe alloy coating has a homogeneous thickness of 3 mm. The chemical composition and microstructure were studied with SEM and XRD. Their result showed that the Ni-Cr-Si-B-Fe alloy coating is defect-free and chemical bonded with plain steel substrate. A light band zone of 8 to 10  $\mu\text{m}$  width was between Ni-Cr-Si-B-Fe alloy coating and plain steel substrate. The coating microstructure is a heterogeneous microstructure and changes from the light band zone to the surface of the coating, which is composed mainly of coarse columnar dendrite, needle-like precipitates and scattered eutectic structures. Four regions across the thickness of Ni brazing alloy coating, due to solidification conditions upon hot - dipping, was identified with

distinguished microstructure. In  $\gamma$ -(Fe, Ni) solid solution matrix, the hard phases of CrB, Fe<sub>2</sub>B and Cr<sub>23</sub>C<sub>6</sub> is identified in the coating. Zhu et al. (2011) demonstrated that carbon nanostructures could be synthesized on the Ni-plated YG6 (WC-6 wt% Co) hardmetal substrate by a simple ethanol diffusion flame method. The morphologies and microstructures of the Ni-plated layer and the carbon nanostructures were examined by various techniques including scanning electron microscopy, X-ray diffraction, and Raman spectroscopy. Their results showed that the quality and the graphitization degree of the flame-deposited carbon nanostructures were significantly enhanced with the increase of deposition time. The characteristics (grain size, shape, and distribution) of the Ni catalyst had a crucial influence on the growth of the carbon nanostructures. In addition, due to the unsteady flame and carbon supply during combustion, inhomogeneous carbon nanostructures were fabricated eventually.

## FUTURE OF BRIGHT NICKEL PLATING

The future of nickel plating will be influenced by changes in marketing conditions and technology. Technological developments that have been considered by researchers and electroplating/electroforming practitioners would foster the growth during the near future. These includes long term performance data on multi-layer nickel coatings; decorative plating of stainless steel; zinc/nickel alloy plating; new uses in battery, electronics; plated plastic and electroless nickel process improvements and the implementation of computer controlled manufacturing. The functional uses of nickel, whether as electroplated coatings or electroform artefacts are growing steadily, as the advantages of this metal in its naturally deposited form or as modified by various techniques become evident to design and production engineers (Dennis and Such, 1993). The corrosion resistance of nanocrystalline materials in aqueous solutions is of great importance in assessing a wide range of potential future applications. To date, advance research in the area of nickel plating is still scarce and relatively few studies have addressed this issue.

## Conclusion

Various factors should be considered for the optimal conditions of the plating bath. Measurement of internal stress of a plating deposit is one of the most important factors. An internal stress testing device utilizing a spiral contractometer is known as a testing device which can create similar plating conditions of the high speed electroplating method. The optimal composition of nickel plating bath and the optimal conditions for electrodeposition are required so as to constantly obtain the best plated films. According to the change of the plating bath, addition of

chemicals, removal of impurities, or adjustment of the various conditions such as current density is required as well as predicting the change in the plating bath composition. To this end, it is necessary to understand, very well, the conditions of a fresh nickel plating solution and the plating solution already in use.

**Abbreviations:** **RS**, Resistance switching; **epi-NiO**, epitaxial NiO; **Tes**, top electrodes; **TEM**, transmission electron microscopy; **SEM**, scanning electron microscope; **UV**, ultraviolet; **ACIS**, 3D modelling kernel/engine; **LIGA**, mask fabrication process; **CSM**, continuous stiffness measurement; **XRD**, X-ray diffraction; **UV-LIGA**, ultraviolet mask fabrication process; **MEMS**, micro-electro-mechanical systems; **EDS**, energy-dispersive X-ray spectroscopy; **MMCs**, metal matrix composites; **LENS**, Laser engineered net-shaping; **EFTEM**, energy-filtering transmission electron microscopy; **EELS**, electron energy-loss spectroscopy; **XPS**, X-ray photoelectron spectroscopy; **RBS**, Rutherford back scattering.

## REFERENCES

- Baek DC, Park TS, Lee SB (2004). Measurement of mechanical properties of electroplated nickel thin film. *Key Eng. Mater.*, 261: 417-422.
- Basrour S, Robert L (2000). X-ray characterization of residual stresses in electroplated nickel used in LIGA technique. *Mat. Sci. Eng.*, 288(2): 270-274.
- Begis YK, Babadzhanyan LS (1996). Coulometric thickness gauges and metrological assurance. *Measurement Techniques*, 39(3): 266-273.
- Davis JR (2000). Nickel, Cobalt and their alloys. ASM international Hand book committee, USA, pp. 107- 108.
- Dennis JK, Such TE (1993). Nickel and chromium plating. Woodhead Publishing. England. pp. 3-5.
- Durney LJ (1984). Electroplating Engineering handbook. Forth Edition, Springer, New York, pp. 315-320.
- Druesne F, Afzali M (2003). Electroplating simulation and design tools. *Proceeding of Institution of Mechanical Engineers, Part B: J. Eng. Manuf.*, 217(5): 705-707.
- Druesne F, Paumelle P, Villon P (2000). Application of the BEM to chromium electroplating simulation and to identification of experimental polarization laws. *Eng. Anal. Boundary Elements*. 24(9): 615-622.
- Fritz T, Cho HS, Hemker KJ, Mokwa W, Schnakenberg U (2002). Characterization of electroplated nickel. *Microsystem Technol.*, 9: 87-91.
- Godinho V, Fernández-Ramos C, Martínez-Martínez D, García-López J, Sánchez-López JC, Fernández A (2008). Microstructural and chemical characterisation techniques for nanostructured and amorphous coatings, *European Phys. J. Appl. Phys.*, 43: 333-341.
- Haimovich J, Leibold K, Staudt G (1996). Estimating and measuring thickness of thin layers by Monte carol simulation and backscattered electron image analysis. *AMP J. Techn.*, 5: 65-78.
- Kakuda TR, Limarga AM, Bennett TD, Clarke DR (2009). Evolution of thermal properties of EB-PVD 7YSZ thermal barrier coatings with thermal cycling, *Acta Materialia* 57: 2583-2591.
- Kaneko Y, Hiwatari Y, Ohara K, Asa F (2006). Monte Carlo simulation of damascene electroplating: Effect of additives. *Molecular Simulation*, 32(15): 1227-1232.
- Karavaev VI, Korobova IL, Litovka YV (2006). Calculation of most uniform electroplated coating with account of changes in the concentration of the electrolyte components. *Russian J. Appl. Chem.*, 79(11): 1820-1824.
- Kim SH (2006). Determination of mechanical properties of electroplated Ni thin film using the resonance method. *Materials Letters*, 61(17): 3589-3592.

- Kim SH, Kang SW (2008). Sensitivity of electroplating conditions on young's modulus of thin film. *Japanese J. Appl. Phys.*, 47: 7314-7316.
- Lee SR, Kim HM, Bak JH, Park YD, Char K, Park HW, Kwon DH, Kim M, Kim DC, Seo S, Li X S, Park GS, Jung R (2010). Investigation of Interface Formed between Top Electrodes and Epitaxial NiO Films for Bipolar Resistance Switching. *Japanese J. Appl. Phys.*, 49(3): 31102-31106.
- Li HY, Huang C, Zeng HP, Jiang KY (2011). Experimental study of Bipolar Pulse Electroforming on Micro Optical Aspheric Mold manufacturing. *Advanced Material Research*, 154: 806-809.
- Lin CS, Lee HB, Hsieh SH (2000). Microstructure and Formability of ZnNi Alloy Electrodeposited Sheet Steel. *Metallurgical Mat. Trans., A* 31(2): 475-485. 35
- Lin T, Wang L, Gao S, Guo Z (2012). Ni-Based Coating on Plain-Carbon Steel by Hot Dipping Process. *Advance Material Research* 361-361: 609-614.
- Luo JK, Pritschow M, Flewitt AJ, Spearing SM, Fleck NA, Milne WI (2006). Effects of Process Conditions on Properties of Electroplated Ni Thin Films for Microsystem Applications. *J. Electrochem. Soc.*, 153(10): D155-D161.
- Mathias FM, Chapman TW (1990). A Zinc-Nickel Alloy Electrodeposition Kinetics Model from Thickness and Composition Measurements on the Rotating Disk Electrode. *J. Electrochem. Soc.*, 137(1): 102-110.
- Ming PM, Zhu D, Zhou F, Hu YY (2010). Vacuum Micro-Electroforming Technique for the production of Void Free Microcomponent. *Key Eng. Mater.*, 426: 142-145.
- Ming PM, Li YJ, Jiang WJ (2011). Morphology and Microhardness of Nickel electroformed under vacuum-degassing conditions. *Key Eng. Mater.*, 455: 495-498.
- Nauenheim C, Kuegeler C, Ruediger A, Waser R (2010). Investigation of the electroforming process in resistively switching TiO<sub>2</sub> nanocrosspoint junctions. *Appl. Phys. Letter*, 96(12): 122902-122905.
- Razeeb MK, Rhen FMF, Roy S (2009). Magnetic properties of nickel nanowires: Effect of deposition temperature. *J. Appl. Phys.*, 105(8): 083922-083922-7.
- Sadiku-Agboola O, Sadiku ER, Ojo OI, Akanji OL, Biotidara OF (2011). Influence of operation parameters on metal deposition in bright nickel-plating process. *Portugaliae Electrochimica Acta.*, 29(2): 91-100.
- Slepishkin VV, Rublinetskaya YV, Stifatov BM (2005). Local Electrochemical Surface Analysis. *J. Analytical Chem.*, 60(2): 120-123.
- Sohn YH, Jayaraj B, Laxman S, Franke B, Byeon JW, Karlsson AM (2004). The Non-Destructive and Nano-Microstructural Characterization of Thermal-Barrier Coatings, *JOM J. Minerals, Metals Mat. Soc.*, 56(10): 53-56.
- Sung-Ting C, Hsien-Chung H, Szu-Jung P, Wen-Ta T, Pee-Yew L, Chung-Hsin Y, Mau-Bin W (2008). Material characterization and corrosion performance of nickel electroplated in supercritical CO<sub>2</sub> fluid. *Corrosion Sci.*, 50(9): 2614-2619.
- Svensson H, Angenete J, Stiller K (2004). Microstructure of oxide scales on aluminide diffusion coatings after short time oxidation at 1050 °C. *Surface Coatings Technol.*, 177-178: 152-157.
- Tang J, Wang H, Guo X, Liu R, Dai X, Ding G, Yang C (2010). An investigation of microstructure and mechanical properties of UV-LIGA nickel thin films electroplated in different electrolytes. *J. Micromechanics Microeng.*, 20(2): 025033.
- Tang J, Wang H, Liu R, Li X, Zhang Z, Yao J, Ding G (2010). A directly strain measuring method for electroplated nickel micro-tensile test. *Microsystem Technol.*, 16(11): 1839-1844.
- Wei X, Lee CH, Jiang Z, Jiang K (2008). Thick photoresists for electroforming metallic microcomponents. *J. Mech. Eng. Sci.*, 222(1): 37-42.
- Zhang X, Long S, Ma Z, Pan Y, Zhou Y (2007). Cup-drawing formation of steel sheet with nickel coating by finite element method. *Trans. Nonferrous Met. Soc. China*, 17: 37-40.
- Zheng B, Topping T, Smugeresky JE, Zhou Y, Biswas A, Baker D, Lavernia EJ (2010). The Influence of Ni-Coated TiC on Laser-Deposited IN625 Metal Matrix Composites. *Metallurgical Materials Trans. A*, 41(3): 567-573.
- Zhu H, Kuang T, Zhu B, Lei S, Liu Z, Ringer SP (2011). Flame synthesis of carbon nanostructures on Ni-plated hardmetal substrates. *Nanoscale Res. Letter*, 6(1): 331-336.